

**METHODS OF EXTRATERRESTRIAL MATERIALS ANALYSIS USING RAMAN SPECTROSCOPIC IMAGING.** M. Fries and A. Steele, Geophysical Laboratory, Carnegie Institution of Washington, 5251 Broad Branch Rd. NW, Washington, D.C. 20015, [m.fries@gl.ciw.edu](mailto:m.fries@gl.ciw.edu).

**Introduction:** Raman spectroscopic imaging is an emerging technique in the analysis of extraterrestrial materials ranging from returned cometary samples [1] to meteorites [2], interplanetary dust (IDPs) [3] and terrestrial impact-derived materials [4]. When performed carefully, Raman imaging can produce material characterization information to include phase identification, some compositional information, alignment of crystalline phases, and the presence and structure of all carbon polymorphs. This data can be collected in a non-destructive manner even on very small particles.

**Analytical Methods:** With modern instrumentation, collection of Raman imagery can be performed with collection time measured from minutes to hours, with pixel sizes well below  $1 \mu\text{m}^2$ .

**Laser Power Measurement.** The relatively weak nature of the Raman effect requires high laser flux which can damage small samples or those with temperature-sensitive phases such as sulfides or high P,T metastable phases. Traditionally, laser power has been reported as the total flux as measured at the focal plane. Given that modern Raman instruments utilize a variety of optical magnification values, a better way to monitor and report laser power is as power density affecting the sample. Lacking the capability to directly measure the distribution of laser power across sub-micron spots, we propose that this value is calculated using a series of approximations. Rayleigh's criterion for focal spot size is used to find the image pixel size for a given magnification and excitation laser wavelength. The laser spot is assumed to have a diameter equal to this spot diameter, laser power is equally distributed across the resulting disk, and the resulting value is given in terms of  $\text{W}/\text{cm}^2$ . While not perfect, this method allows direct comparison of laser power subjected to a sample between different Raman devices, objective lens magnification, and excitation laser wavelength.

**Laser Power Constraints.** In order to place constraints on laser power such that fragile samples are not damaged in the course of measurement, a standardized characterization method is proposed. Scrapings of troilite from the Toluca iron meteorite are prepared and pressed into gold foil. A minimum of three roughly micron-sized troilite flakes was subjected to increasing laser power density until the troilite-pyrrhotite transition was observed in its Raman spectrum. The calculated laser power density that initiated this transition is then set as the maximum power density allowed for

analysis of returned cometary material, IDPs and other materials that contain fine-grained sulfides. For the WITec  $\alpha$ -SNOM device used here, a power density of  $32.9 \text{ kW}/\text{cm}^2$  was calculated as the upper limit using this technique.

This method should ensure that sulfides and other fragile mineral phases are not damaged during Raman analysis. It must be noted that this technique assumes that any fine-grained or other fragile sample materials are in intimate contact with other materials that function as a suitable heat sink. Especially "fluffy" materials require special consideration and may not be suitable for Raman analysis. Additionally, the upper power limit value measured using this technique is specific to each Raman instrument due to vagaries of focusing optics. Troilite used for this method can originate from any iron meteorite or a prepared standard.

**Mineralogical Imaging.** Using Raman spectroscopic imaging to identify mineral phases is the most basic use of Raman spectroscopy and is especially useful in the form of images (Figure 1A). Most Raman spectra are composed of first-order peaks only, simplifying the task of spectral deconvolution to produce single-phase maps. Mapping the intensity of a single peak particular to the peak in question can make a map of a single phase. Other methods of separating phases include thresholding a peak center in the case of two or more phases which produce Raman peaks of nearly the same Raman shift, such as the ca.  $670 \text{ cm}^{-1}$  peak found in magnetite, pyroxenes, jarosite and others. In a case where phases share a peak but one exhibits at least one other prominent peak, a negative mask can be assembled from the intensity the alternative peak. The resulting mask is applied to the shared peak image to produce an image of the single-peak phase. Manual selection is useful mostly as a refinement technique and should be avoided for producing phase images from scratch. RGB composite images can also be assembled to demonstrate the spatial interrelationship of selected phases. Reflectance imaging is also useful, as it produces a monochromatic image of the sample surface simply by producing an image from the intensity of the reflected excitation laser.

**Phase Composition.** Many mineral phases that can accommodate changes in cation composition can be imaged with regard to their composition. Changes in cation composition cause variation in unit cell parameters and their attendant vibrational energies, which are manifested as a peak center shift in Raman

modes (Figure 1B). Spinel-type minerals, olivine, some sulfides and to some extent pyroxenes have been characterized in this regard [5-7]

**Crystalline Orientation.** Many phases, particularly phases exhibiting crystallographic anisotropy, produce Raman spectral peaks that vary in intensity with regard to crystallographic orientation to the excitation laser. The ratio of variant/invariant peaks or mutually invariant peaks will produce an image of the relative crystallographic orientation of the phase (Figure 1C).

**Carbon Imaging Characterization.** All polytypes of carbon can be detected and characterized by Raman spectroscopy. The form of carbon most abundant in extraterrestrial materials is macromolecular carbon (MMC), which is a term that describes a condensed, disordered carbon material with some degree of microcrystalline order and can vary from nearly amorphous carbon to lightly altered graphite. MMC can be characterized in terms of the ordered fraction, which is sometimes referred to as the “graphitic” fraction. A Raman spectrum of MMC [8] predominantly features the disordered (D) and “graphitic” (G) bands at around 1350 and 1590  $\text{cm}^{-1}$  respectively. Tuinstra and Koenig [8] have shown that the G/D intensity ratio is proportional to the average diameter of ordered domains in the C crystallographic direction ( $L_C$ ) where an amorphous carbon material exhibits  $L_C=0$  and graphite is essentially a continuous unit cell with  $L_C=\infty$ . This finding was refined by Matthews et al [9] to accommodate changes in response to excitation laser wavelength.

With nucleation and growth of ordered domains in carbon comes a distribution of domain size with respect to the number of domains. A single Raman spectrum of MMC is essentially integrated over the domain size distribution found within a single focal spot. By collecting a large number of Raman spectra of a target MMC, the curve representing the ensemble of domain sizes in the bulk material can be reconstructed from a histogram of G/D intensity values from individual spectra (Figure 1D). This distribution is sensitive to the thermal history of MMC and can be deconvolved to quantitatively express heterogeneity within the MMC. This technique is uniquely applicable to extraterrestrial MMC from a variety of sources to quantitatively express thermal processing in the parent material.

**Summary:** Raman imaging is a highly versatile technique for analysis of extraterrestrial materials that complements more customary techniques. Phase identification and characterization that may include crystallographic orientation, composition and grain size distribution are attainable in spatial context using Raman imaging techniques.

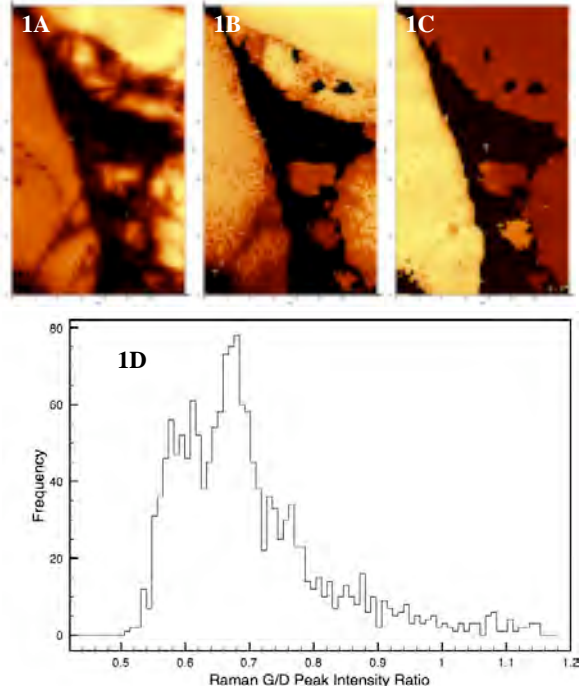


Figure 1A) Raman image of olivine  $\sim 850 \text{ cm}^{-1}$  peak intensity from a chondrule in the QUE 94366 carbonaceous chondrite. Image size is  $30 \times 50 \mu\text{m}$ . 1B) Olivine relative iron content image, where darker color indicates more fayalitic olivine. 1C) Olivine orientation image from same field as 1A. Note the small polycrystalline grain in the center of the image as revealed by multiple orientation domains. 1D) histogram of carbon G/D intensity values for a MMC example.

**References:** [1] Sandford S. and 54 co-authors (2006) *Science* 314, 5806, 1720-1724. [2] Fries M., Steele A., and McCoy T. (2005) 68<sup>th</sup> MetSoc Abstract #5302. [3] Wopenka, B., (1988) *EPSL* 88, 3-4, 221-231. [4] McHone J., Fries M., Steele A. (2005) 36<sup>th</sup> LPSC, Abstract #2315. [5] Wang A., Kuebler K. E., Jolliff B. L., Haskin L. A., (2003) 34<sup>th</sup> LPSC, Abstract #1742. [6] Wang A., Jolliff B. L., Viskupic K. M., Haskin L. A., (1997) 28<sup>th</sup> LPSC P1491-1492. [7] Fries M., Boctor N., Steele A., unpublished data. [8] Tuinstra F., Koenig J. (1970), *J. Chem. Phys.* 53, 1126-1130. [9] Matthews M. et al. (1999) *Phys. Rev. B* 59, R6585-R6588